

Numerical determination of bound states without matrix diagonalization

D Waxman

Centre for Theoretical Physics and Centre for the Study of Evolution, The University of Sussex, Brighton, Sussex BN1 9QJ, UK

Received 11 September 1997, in final form 11 November 1997

Abstract. We present a simply applied numerical technique that allows the accurate determination of the bound-state eigenfunctions and eigenvalues of a differential operator such as the one-particle Schrödinger Hamiltonian. The method applies for potentials that asymptotically vanish. The eigenvalues and eigenfunctions are determined as functions of the strength of the potential and the method is able to determine the bound-state energies for arbitrarily weak strengths of the potential. At no point is a matrix diagonalized thus the method may be applied to problems with space dimension greater than unity.

1. Introduction

In this work a numerical technique is presented that determines the bound-state eigenvalues (assumed discrete) of linear differential operators such as the Schrödinger Hamiltonian of one-particle quantum mechanics. Other operators for which the method applies are matrix differential operators such as first quantized Dirac or Bogoliubov Hamiltonians. The method determines the bound-state energy eigenvalues and the associated eigenfunctions once the potential is specified.

One virtue of this work is the simplicity with which it may be implemented. All that is required is iteration of an integral equation which, when discretized, becomes a matrix equation. Since the iteration has good convergence properties it is never necessary to diagonalize a matrix.

A second virtue is that, provided the potential vanishes rapidly (e.g. exponentially) the bound-state eigenvalues and eigenfunctions may be determined to high accuracy, irrespective of the weakness of the potential. This is a highly non-trivial feature of the method we present since very weak potentials have bound states which typically extend very great distances beyond the region where the potential is non-zero and it is often hard to accurately determine the eigenfunctions and eigenvalues in this situation.

2. Method for the ground state

To describe the method in its simplest form, we consider the one-dimensional Schrödinger eigenvalue equation ($\partial_x \equiv \partial/\partial x$)

$$[-\partial_x^2 - \lambda V(x)]u(x) = -\epsilon u(x) \quad (1)$$

$$\lim_{|x| \rightarrow \infty} u(x) = 0 \quad (2)$$

where we have written the potential as $-\lambda V(x)$ and $\lambda (> 0)$ is a parameter that determines the strength of the potential. Henceforth we shall call λ the ‘strength of the potential’.

In this work, we consider potentials $-\lambda V(x)$ that are attractive (< 0) for some x and which vanish as $|x| \rightarrow \infty$. The energy eigenvalue in (1) has been written as $-\varepsilon$ with $\varepsilon > 0$, hence the eigenvalue is negative and corresponds to a bound state.

Let us write (1) as

$$[-\partial_x^2 + \varepsilon]u(x) = \lambda V(x)u(x) \quad (3)$$

and introduce the Green function $G_\varepsilon(x)$ that obeys

$$[-\partial_x^2 + \varepsilon]G_\varepsilon(x) = \delta(x) \quad (4)$$

$$\lim_{|x| \rightarrow \infty} G_\varepsilon(x) = 0. \quad (5)$$

Then (1) and (2) are equivalent to

$$u(x) = \lambda \int_{-\infty}^{\infty} G_\varepsilon(x-x')V(x')u(x') dx'. \quad (6)$$

Note that no solution to the homogeneous equation, $[-\partial_x^2 + \varepsilon]u(x) = 0$, can be added to the right-hand side of (6) since such a solution will not vanish for at least one of the two limits $x \rightarrow -\infty$ or $x \rightarrow \infty$.

So far we have not specified a normalization of $u(x)$; a convenient choice is

$$u(x_{\text{ref}}) = 1 \quad (7)$$

where x_{ref} is arbitrary. Making the choice $x_{\text{ref}} = 0^\dagger$ and substituting this value into (6) allows λ to be written as

$$\lambda = \frac{1}{\int G_\varepsilon(x')V(x')u(x') dx'}. \quad (8)$$

Using this equation to eliminate λ from (6) yields

$$u(x) = \frac{\int G_\varepsilon(x-x')V(x')u(x') dx'}{\int G_\varepsilon(x')V(x')u(x') dx'}. \quad (9)$$

Equations (8) and (9) are the starting point from which a rapidly convergent iteration scheme may be formulated for the lowest energy bound state (excited states may also be obtained—see later). The procedure is slightly indirect in that we solve an inverse problem: we do not determine the eigenvalue, $-\varepsilon$, as a function of λ , but rather λ as a function of ε . Thus we make a particular choice for ε , iterate the equation

$$u_{n+1}(x) = \frac{\int G_\varepsilon(x-x')V(x')u_n(x') dx'}{\int G_\varepsilon(x')V(x')u_n(x') dx'} \quad (10)$$

until it converges to $u(x) \equiv u_\infty(x)$ and then use the $u_\infty(x)$ obtained from this procedure to determine the value of λ , using (8). In this way we determine the strength of the potential, λ , that leads to a bound state of energy $-\varepsilon$, i.e. we find $\lambda(\varepsilon)$. Repeating the process for a set of different values of ε , say $[\varepsilon_1, \varepsilon_2, \dots, \varepsilon_n]$ yields a set of potential strengths, $[\lambda_1, \lambda_2, \dots, \lambda_n]$ and at this point we can infer the dependence of ε on λ by e.g. making a plot of ε against λ or by numerically interpolating the results.

Before we give a proof of the convergence of (10), we note that the iteration scheme of (10) can be formulated for two somewhat different cases.

[†] Sometimes (e.g. with symmetric potentials) the choice $x_{\text{ref}} = 0$ may cause problems since the very function we are trying to determine may vanish at this point. In this case another choice for x_{ref} should be made.

(i) For the first case, the potential is appreciably different from zero only for a finite range of x . This would apply to attractive potential wells where the potential vanishes beyond a certain range. Alternatively, potentials that fall rapidly to zero with $|x|$ (e.g. as an exponential of $|x|$) can be treated by setting the potential strictly to zero for $|x|$ larger than some length a . The length a is chosen so that computed quantities do not change, to a given numerical accuracy, when a is increased. A feature of this case (i.e. potentials effectively vanishing beyond a certain range) is that knowledge of the eigenfunction is only required in the region of x where $V(x)$ is effectively non-zero. This follows since, on the right-hand side of (10), only the combination $V(x')u_n(x')$ is present. We thus use (10) to directly determine $u(x)$ only in this range. Outside this range we can determine the eigenfunction using (6), since for a given ε , the quantities λ and $u(x)$ (in the region where $V(x)$ is effectively non-zero) are determined via iteration, so all information needed for (6) is known and we can determine $u(x)$ at all points. It follows that the virtue of calculating $u(x)$ only in the region of non-zero $V(x)$ is that e.g. weakly bound states may extend very great distances beyond the range of the potential but the information contained in the long tails is essentially trivial and need not be followed numerically.

(ii) The second case occurs when the bound-state eigenfunction becomes negligible for sufficiently large $|x|$, say $|x| \geq a$. The integration in (10) can then be terminated at $|x| = a$. For this case, convergence of the integrals appearing on the right-hand side of (10) is controlled by the behaviour of the eigenfunction and it thus allows the treatment of problems where the potential does not fall rapidly to zero. One example is the s-wave radial problem for the Coulomb potential. Later in the paper we give numerical results for this potential, which is a numerically interesting case, because of the singular nature of the potential.

A variety of the linear operators met in physics yield an integral equation for bound states that can be written in the same form as (9). Once this form is established, all that is needed to determine bound states and their eigenvalues is the 'free' (i.e. $V = 0$) Green function.

To put our work in context, we note that a related paper is [1] where an integral equation ('heat kernel') method was used to convert the Schrödinger equation to an integral equation, which was then used to extract bound states. The method of this reference suffers (in the case of the Hydrogen atom) with slow convergence to the ground state and yields results of less than ideal numerical accuracy. In [2], the results of [1] were improved using extrapolation techniques that accelerated its convergence. A second relevant piece of work is [3], where the Lippmann–Schwinger equation is treated in an N level approximation. This method appears to have limitations on the accuracy of the results it produces. The last related piece of work we shall mention is [4], where the strength of the potential yielding a bound state with a specified number of nodes and a specified energy was determined. The method of [4] required the numerical integration of the Schrödinger equation from the left and the right and as already noted, this may be problematic in the case of weakly bound states. Additionally, the generalization of the method of [4] to non-symmetric potentials in dimensions greater than unity or to different differential operators is not obvious.

The method we present in this work generally yields very rapid convergence to the ground state and does not require any special treatments of convergence. It yields eigenvalues and eigenfunctions to high numerical accuracy for both weakly and non-weakly bound states and possesses natural generalizations to operators other than those of Schrödinger type.

3. Proof of convergence to the ground state

In this section we shall prove convergence of the iteration scheme of (10) to the ground state using Dirac notation. We shall only provide a proof of convergence to the ground state for the one-dimensional Schrödinger operator considered in the previous section but with the necessary changes, the proof can be extended to other operators.

To proceed with the proof, we start with (10) which, in Dirac notation is

$$|u_{n+1}\rangle = \frac{G_\varepsilon V |u_n\rangle}{\langle 0 | G_\varepsilon V |u_n\rangle} \quad (11)$$

where $\langle 0 |$ is an eigenstate of the x -coordinate operator with eigenvalue 0 and[†]

$$G_\varepsilon = (p_x^2 + \varepsilon)^{-1}. \quad (12)$$

Then

$$|u_1\rangle = \frac{G_\varepsilon V |u_0\rangle}{\langle 0 | G_\varepsilon V |u_0\rangle} \quad |u_2\rangle = \frac{G_\varepsilon V |u_1\rangle}{\langle 0 | G_\varepsilon V |u_1\rangle} = \frac{(G_\varepsilon V)^2 |u_0\rangle}{\langle 0 | (G_\varepsilon V)^2 |u_0\rangle}$$

and generally

$$|u_{n+1}\rangle = \frac{(G_\varepsilon V)^{n+1} |u_0\rangle}{\langle 0 | (G_\varepsilon V)^{n+1} |u_0\rangle}. \quad (13)$$

Consider now the right eigenvector, $|\phi\rangle$, of $G_\varepsilon V$ that is associated with eigenvalue $\frac{1}{\mu}$:

$$G_\varepsilon V |\phi\rangle = \frac{1}{\mu} |\phi\rangle. \quad (14)$$

Note that the behaviour of $G_\varepsilon(x)$ at large $|x|$, (5), ensures that $\phi(x) \equiv \langle x | \phi \rangle$ obeys

$$\lim_{|x| \rightarrow \infty} \phi(x) = 0. \quad (15)$$

Using the definition of (12) allows (14) to be written as

$$(p_x^2 - \mu V) |\phi\rangle = -\varepsilon |\phi\rangle. \quad (16)$$

This result, combined with (15), tells us that $|\phi\rangle$ is a *bound* state of the potential $-\mu V$. The possible values of μ correspond to the different strengths of the potential that all lead to a bound-state at the same energy, namely $-\varepsilon$. The vector $|\phi\rangle$ may therefore be the ground state or an excited state of the potential $-\mu V$ and only by choosing μ appropriately will the energy of the state be $-\varepsilon$. Let μ_0 be the smallest value of μ that leads to a bound state with energy $-\varepsilon$ and let the eigenvector associated with μ_0 be $|\phi_0\rangle$. The fact that μ_0 is the smallest value of μ that results in a bound state means that $|\phi_0\rangle$ must be the ground state of the potential $-\mu_0 V$. The next smallest value of μ , namely μ_1 , corresponds to an eigenvector $|\phi_1\rangle$ (with energy $-\varepsilon$) that is the first excited state of the potential $-\mu_1 V$. Larger values of μ correspond to $|\phi\rangle$'s that are higher excited states of the potential $-\mu V$. This reasoning indicates that μ only takes on a *discrete* set of values, μ_0, μ_1, \dots

Let us write

$$G_\varepsilon V = \sum_{s=0}^{\infty} |\phi_s\rangle \frac{1}{\mu_s} \langle \psi_s | \quad \langle \psi_r | \phi_s \rangle = \delta_{rs} \quad (17)$$

[†] We thus normalize the eigenfunction so that $u(0) = 1$. More generally we will write the normalization condition as $\langle \text{ref} | u \rangle = 1$ where $\langle \text{ref} |$ is a suitable reference vector. If the method described here is applied to a matrix differential operator such as a Dirac Hamiltonian, then $\langle \text{ref} |$ will incorporate spinor structure as well as containing e.g. eigenvectors of the coordinate operator.

where † δ_{rs} a Kronecker delta ‡.

Although $|u_0\rangle$ will generally not be representable as a superposition over the set $\{|\phi_s\rangle\}$, since $\{|\phi_s\rangle\}$ does not generally constitute a complete set, we can write

$$|u_1\rangle = \frac{\sum_s |\phi_s\rangle \frac{1}{\mu_s} \langle \psi_s | u_0 \rangle}{\sum_s \langle 0 | \phi_s \rangle \frac{1}{\mu_s} \langle \psi_s | u_0 \rangle} \stackrel{\text{def}}{=} \sum_{s=0}^{\infty} c_s |\phi_s\rangle \tag{18}$$

where c_s are coefficients that are determined by $|u_0\rangle$.

Application of (13) yields

$$|u_{n+1}\rangle = \frac{\sum_s c_s \mu_s^{-n} |\phi_s\rangle}{\sum_s c_s \mu_s^{-n} \langle 0 | \phi_s \rangle} \tag{19}$$

thus as long as $c_0 \neq 0$, we have

$$\begin{aligned} |u_{n+1}\rangle &= \frac{c_0 |\phi_0\rangle + \sum_{s=1}^{\infty} c_s \left(\frac{\mu_0}{\mu_s}\right)^n |\phi_s\rangle}{c_0 \langle 0 | \phi_0 \rangle + \sum_{s=1}^{\infty} c_s \left(\frac{\mu_0}{\mu_s}\right)^n \langle 0 | \phi_s \rangle} \\ &= \frac{|\phi_0\rangle}{\langle 0 | \phi_0 \rangle} + \mathcal{O}\left(\left(\frac{\mu_0}{\mu_1}\right)^{n+1}\right). \end{aligned} \tag{20}$$

We thus have exponential convergence to the state $|\phi_0\rangle$ which is the ground state of the potential $-\mu_0 V$. Additionally, the value of λ , computed from (8) after convergence has been achieved, is μ_0 .

4. Determination of higher bound states

The reason the iteration of (10) converges to the ground state is that in (17), $1/\mu_0$ is the largest eigenvalue of $G_\varepsilon V$. We can ensure convergence to the first excited bound state by performing the iteration with the operator

$$M_1 \stackrel{\text{def}}{=} G_\varepsilon V - |\phi_0\rangle \frac{1}{\mu_0} \langle \psi_0 | \equiv \sum_{s \neq 0} |\phi_s\rangle \frac{1}{\mu_s} \langle \psi_s |. \tag{21}$$

Thus the difference equation

$$|u_{n+1}\rangle = \frac{M_1 |u_n\rangle}{\langle 0 | M_1 |u_n\rangle} \tag{22}$$

will converge to $|u_\infty\rangle = |\phi_1\rangle / \langle 0 | \phi_1 \rangle$, the first excited bound state (with energy $-\varepsilon$) of the potential $-\mu_1 V$ where $\mu_1 = 1 / \langle 0 | M_1 |u_\infty\rangle \equiv \langle 0 | \phi_1 \rangle / \langle 0 | M_1 | \phi_1 \rangle$.

One possible way of determining the projection operator $|\phi_0\rangle \frac{1}{\mu_0} \langle \psi_0 |$ is to iterate the ‘left’ equation $\langle v_{n+1} | = \frac{\langle v_n | G_\varepsilon V}{\langle v_n | G_\varepsilon V | 0 \rangle}$ to convergence. This yields $\langle v_\infty | \equiv \frac{\langle \psi_0 |}{\langle \psi_0 | 0 \rangle}$ and since $\frac{|\phi_0\rangle}{\langle 0 | \phi_0 \rangle}$ and μ_0 have already been found, the projection operator may be immediately constructed from these.

Higher excited states may be similarly found by constructing M_2, M_3, \dots where $M_n = G_\varepsilon V - \sum_{s=0}^{n-1} |\phi_s\rangle \frac{1}{\mu_s} \langle \psi_s |$.

† We use the notation $\langle \psi_s |$ to denote the left eigenvector of $G_\varepsilon V$ belonging to eigenvalue $1/\mu_s$. $\langle \psi_s |$ is not the dual (‘conjugate’) of the right eigenvector belonging to the same eigenvalue, $|\phi_s\rangle$, since $G_\varepsilon V$ is not a Hermitian operator.

‡ We have written the values of s ranging from 0 to ∞ , however the set of eigenvalues of $G_\varepsilon V$ may be finite in which case the sum over s should terminate at a finite value.

5. Illustrative examples

5.1. Double delta function potential in one dimension

A single delta function potential converges in one iteration of (10) to the exact (and unique) bound state of the potential. More interesting and illuminating is the case of the double delta function potential

$$-\lambda V(x) = -\lambda[\delta(x-a) + \delta(x+a)] \quad (23)$$

whose bound states can, of course, be found in closed form.

The decomposition $G_\varepsilon V = \sum_s |\phi_s\rangle \frac{1}{\mu_s} \langle \psi_s|$ has, in this case, only two terms in it: $s = 0$ and $s = 1$ and a straightforward calculation shows

$$\mu_0 = \frac{2\sqrt{\varepsilon}}{1 + e^{-2\sqrt{\varepsilon}a}} \quad \mu_1 = \frac{2\sqrt{\varepsilon}}{1 - e^{-2\sqrt{\varepsilon}a}}. \quad (24)$$

Thus the action of $G_\varepsilon V$ on an arbitrary initial function, $u_0(x)$ first projects it into the two-dimensional space of bound states, $\phi_0(x) = \exp(-\sqrt{\varepsilon}|x-a|) + \exp(-\sqrt{\varepsilon}|x+a|)$ and $\phi_1(x) = \exp(-\sqrt{\varepsilon}|x-a|) - \exp(-\sqrt{\varepsilon}|x+a|)$ and in each subsequent iteration the relative contribution of $\phi_1(x)$ is reduced by a factor

$$\frac{\mu_0}{\mu_1} = \tanh(\sqrt{\varepsilon}a). \quad (25)$$

This result shows that small values of ε lead to the most rapid convergence to the ground state.

5.2. $\text{sech}^2 x$ potential

Another example that has analytically known eigenvalues and provides a further example of the method presented in this work is the potential $-\lambda V(x) = -\lambda \text{sech}^2 x$. This potential vanishes exponentially for large $|x|$ and may be set to zero at large $|x|$ with negligible influence on the bound states calculated. The bound-state eigenvalues of the potential are known in closed form [5]. They satisfy

$$(p_x^2 - \lambda V)|\phi\rangle = -\varepsilon_m |\phi\rangle. \quad (26)$$

with

$$\varepsilon_m = \left(\sqrt{\frac{1}{4} + \lambda} - \frac{1}{2} - m \right)^2 \quad (27)$$

$$m = 0, 1, 2, \dots, \left[\sqrt{\frac{1}{4} + \lambda} - \frac{1}{2} \right]$$

and $[\alpha]$ denotes the largest integer $\leq \alpha$.

Let us now view (26) and (27) from the alternative perspective of this work and imagine that the bound-state energy $-\varepsilon$ is specified. Then the ‘quantized’ strengths of the potential, μ_s , that lead to the specified bound-state energy are

$$\mu_s = (\sqrt{\varepsilon} + s)(\sqrt{\varepsilon} + s + 1) \quad s = 0, 1, 2, \dots \quad (28)$$

A convenient way to see the convergence of the iteration of (10) is to define for the ground state, the effective strength of the potential after n iterations[†]:

$$\lambda_n = \frac{1}{\int G_\varepsilon(x') V(x') u_n(x') dx'}. \quad (29)$$

[†] For the case of states other than the ground state, we define λ_n by replacing $G_\varepsilon V$ in (29) by the appropriate M_n operator, see section 4.

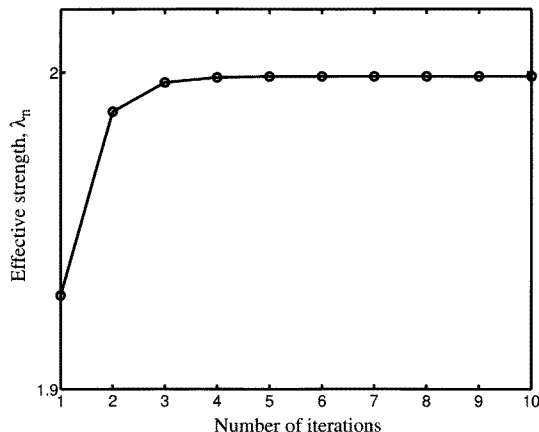


Figure 1. The effective strength of the potential, λ_n , is plotted against iteration number, for $V(x) = \text{sech}^2 x$ when the binding energy of the bound state is $\varepsilon = 1$. The iteration sequence plotted is the one that converges to the ground state. The iteration was initiated with a random function and the space interval $(-3.5, 3.5)$ was discretized into 101 points. The exact value for the strength of the potential is $\lambda_\infty = 2$.

The arguments of section 3 indicate that λ_n behaves as

$$\lambda_n \rightarrow \mu_0 \equiv \sqrt{\varepsilon}(\sqrt{\varepsilon} + 1) \tag{30}$$

when iteration, using $G_\varepsilon V$, is carried out, while if the operator M_1 of (21) is used, it behaves as

$$\lambda_n \rightarrow \mu_1 \equiv (\sqrt{\varepsilon} + 1)(\sqrt{\varepsilon} + 2). \tag{31}$$

To illustrate the above, we have approximated the integral in (10) by using an elementary midpoint integration rule† with 101 space points and plotted the results of iterating (10), when $\varepsilon = 1$. Despite the fact that ε is not small, there is rapid convergence of λ_n to a value that is very close to the exact value of (30), as is illustrated in figure 1. Similarly, replacing $G_\varepsilon V$ by M_1 (see (21)), again for $\varepsilon = 1$, yields rapid convergence to the result of (31), i.e. the strength appropriate for the first excited state, as may be seen in figure 2.

In figure 3 we plot ε as a function of the strength of the potential, λ , for the $\text{sech}^2 x$ potential. We obtain this figure by first calculating the λ 's corresponding to a set of different ε 's (by iterating (10) to convergence). To the eye there is no discernible difference between the exact result ($\varepsilon = (\sqrt{\frac{1}{4} + \lambda - \frac{1}{2}})^2$) and the numerically determined results. For a midpoint integration rule with 101 space points, the exact and numerical results differ by less than 0.1%, for 201 space points the difference is less than 0.04%.

5.3. Random potential

It is also possible to consider random potentials and see effects of localization on the eigenfunctions. As an example, we considered the potential to be non-zero in the space interval $(-1, 1)$ and zero outside this. We took the potential to be $-\lambda V(x)$ with $V(x)$ taken to be uncorrelated at different spatial points and at each spatial point, uniformly distributed in the range $(0, 1)$. To define the problem further we applied a midpoint rule

† By a midpoint integration rule, we mean $\int_0^a f(x) dx \approx \delta \sum_{j=1}^N f((j - \frac{1}{2})\delta)$ with $\delta = a/N$.

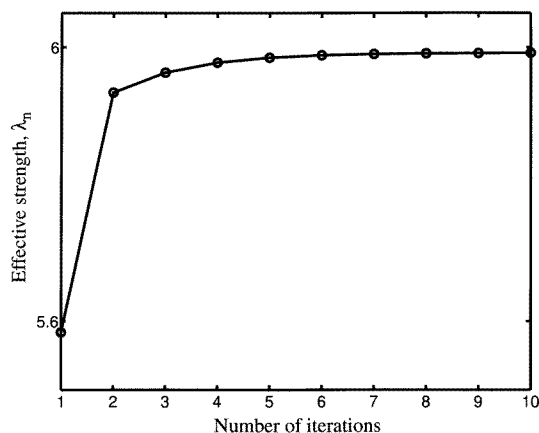


Figure 2. The effective strength of the potential, λ_n is plotted against iteration number, for $V(x) = \text{sech}^2 x$ when the binding energy of the bound state is $\varepsilon = 1$. The iteration sequence plotted is the one that converges to the first excited state. The iteration was initiated with a random function and the space interval $(-3.5, 3.5)$ was discretized into 101 points. The exact value for the strength of the potential is $\lambda_\infty = 6$.

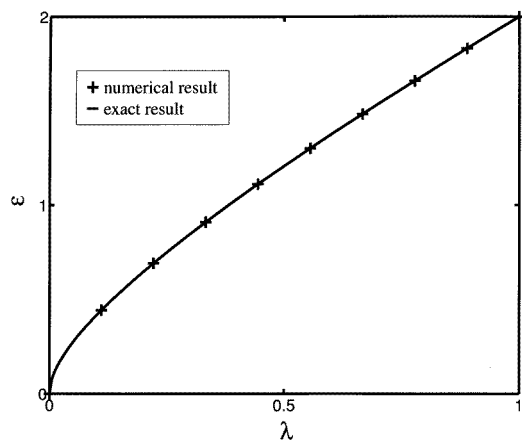


Figure 3. The eigenvalue equation $(-\partial_x^2 - \lambda \text{sech}^2 x)\phi(x) = -\varepsilon\phi(x)$ was solved, using the iteration method of the text, for ε as a function of λ . The points labelled by + are the result of the method of this work and the full curve is the known exact result. The iteration was initiated with a random function when the interval $(-3.5, 3.5)$ was discretized into 201 points.

to the integral equation (10) with 41 spatial points, thus effectively, the potential may be considered piecewise constant over an interval of 0.05. We specified an energy eigenvalue and determined the strength of the potential, λ , and the ground-state eigenfunction. In contrast to the previous cases, it took many iterations to achieve convergence (e.g. as signalled by (29) it sometimes took as many as 500 iterations to achieve λ_n constant from one iteration to the next, to 16 significant digits). This is not surprising since a random potential has many low-lying states and a slight change in the strength of the potential may cause any of these to become the ground state at the specified energy. An alternative way of saying this is that the eigenvalues $1/\mu_s$ of (14) are closely spaced and hence convergence is not rapid.

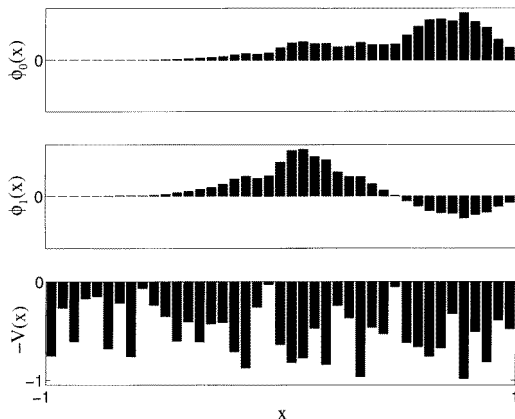


Figure 4. This figure illustrates results for a random potential. Space was discretized into 41 points between -1 and 1 and a random potential was generated at these points. Outside the interval $(-1, 1)$ the potential vanishes. The ground and first excited states in this potential $\phi_0(x)$ and $\phi_1(x)$ are plotted along with the random potential $-V(x)$ used. Note that the eigenfunctions plotted both correspond to an eigenvalue of $-\varepsilon = -225$ but the values of λ (which are a result of the iteration) are different in the two cases. For the ground state, $\lambda = 357.51$ and for the first excited state, $\lambda = 368.14$.

In figure 4 we plot the ground and first excited states, $\phi_0(x)$ and $\phi_1(x)$ along with the random potential $-V(x)$ used. Note that the eigenfunctions plotted both correspond to an eigenvalue of $-\varepsilon = -225$ but the values of λ (which are a result of the iteration) are different in the two cases. For the ground state, $\lambda = 357.51$ and for the first excited state, $\lambda = 368.14$.

5.4. Coulomb potential

The s-wave radial problem associated with the Coulomb potential provides an example of a potential that does not tend rapidly to zero and has the further interesting complication that it is singular at the origin.

If $u(r)$ denotes the eigenfunction for the s-wave problem, then $\chi(r) \equiv ru(r)$ is taken to satisfy

$$\begin{aligned} \left(-\frac{d^2}{dr^2} - \lambda V(r) \right) \chi(r) &= -\varepsilon \chi(r) \\ V(r) &= \frac{2}{r} \\ \chi(0) &= 0 \quad \chi(\infty) = 0. \end{aligned} \tag{32}$$

Exact results for this problem are

$$\chi(r) = r \exp(-\lambda r) \quad \varepsilon = \lambda^2. \tag{33}$$

To numerically treat this problem, we modified (10) to

$$\chi_{n+1}(r) = \frac{\int_0^\infty G_\varepsilon(r, r') V(r') \chi_n(r') dr'}{\int_0^\infty G_\varepsilon(r_{\text{ref}}, r') V(r') \chi_n(r') dr'} \tag{34}$$

where $G_\varepsilon(r, r')$ obeys

$$\begin{aligned} \left(-\frac{d^2}{dr^2} - \lambda V(r)\right) G_\varepsilon(r, r') &= \delta(r - r') \\ G_\varepsilon(0, r') &= 0 \quad G_\varepsilon(\infty, r') = 0. \end{aligned} \tag{35}$$

The singularity of the potential at $r' = 0$ was treated by integrating r' in (34) upwards from 10^{-6} rather than zero. The rapid decrease of the eigenfunction at large r' was used to terminate the r' integral at $r' = 15$. These choices yielded numerically robust results for λ ranging from 0.7 to 1.4 when (34) was discretized and iterated. Splitting the radial interval into 200 parts led to results for λ with an error smaller than 0.6%. With the numerical and exact $\chi(r)$ normalized so that $\text{Max}_r(\chi(r)) = 1$, a global measure of the goodness of the eigenfunction was obtained by evaluating

$$\frac{\int_0^\infty [\chi_{\text{numerical}}(r) - \chi_{\text{exact}}(r)]^2 dr}{\int_0^\infty [\chi_{\text{exact}}(r)]^2 dr}. \tag{36}$$

For the parameters we considered, the value of this quantity was 1.25×10^{-4} or smaller.

5.5. Threshold behaviour

Interesting information about threshold behaviour may also be obtained.

For definiteness let us consider the finite square-well potential

$$-\lambda V(x) = \begin{cases} 0 & x < -1 \\ -\lambda & -1 < x < 1 \\ 0 & x > 1. \end{cases} \tag{37}$$

We can straightforwardly apply the technique of section 4 to determine the strength of the potential that leads to a first excited state of energy $-\varepsilon$. If we now consider progressively smaller values of ε , the value of λ obtained will tend to the smallest value that just binds a particle in the first excited state. The program written to determine the threshold behaviour dealt with the quantity $\sqrt{\varepsilon}$ rather than ε itself and we found, in practise, that allowing $\sqrt{\varepsilon}$ to range from 10^{-7} to 10^{-8} yielded a value of λ that was constant to seven significant figures, allowing a good indication of the threshold value. Note that $\sqrt{\varepsilon} = 10^{-8}$, while being a small number, is still sufficiently large compared with machine precision ($\sim 10^{-16}$) that rounding errors etc do not have any significant effect on the results.

The threshold value of λ in this problem can, of course, be solved exactly. We have that within the well the eigenfunction obeys

$$[-\partial_x^2 - \lambda]u(x) = 0 \quad \left. \frac{du(x)}{dx} \right|_{x=\pm 1} = 0 \tag{38}$$

the derivative condition ensuring that at threshold, $u(x)$ joins smoothly to a constant solution outside of the well. The solution for $-1 < x < 1$ is

$$u(x) = \sin\left(\frac{\pi x}{2}\right) \tag{39}$$

and the threshold value of λ , namely $\lambda_{\text{threshold}}$, such that any larger value of λ will yield an odd-parity bound state, is

$$\lambda_{\text{threshold}} = \left(\frac{\pi}{2}\right)^2. \tag{40}$$

Numerically we obtained the result $(\frac{\pi}{2})^2$ to 0.01% accuracy using a midpoint rule with 101 space points.

5.6. Higher-dimensional case

As we have already noted, it is possible to apply the iteration method to higher-dimensional cases. As an example, consider a two-dimensional problem where the potential is the finite square well

$$-\lambda V(r, \theta) = -\lambda \Theta(1 - r) \quad (41)$$

where $\Theta(r)$ denotes a Heaviside step function. We have chosen this potential since we can readily determine its ground-state eigenvalue and hence test the method. It is, of course, possible to reduce this case to a one-dimensional (radial) problem; we have not done so, but instead have determined the full two-dimensional behaviour of the eigenfunction. We find that for this potential, and, indeed, for non-central potentials such as $V(r, \theta) = \Theta(1 - r) \cos^2 \theta$ with smooth angular behaviour, the iteration converges reasonably rapidly (e.g. for the eigenvalue $\varepsilon = 1$, we find convergence in around 30 iterations). We have achieved accuracies better than 0.1% in $\varepsilon(\lambda)$ when we have used a midpoint rule to evaluate the integrals required, with only 10 radial points and 32 angular points.

6. Discussion

In this work we have presented a simple technique for numerically determining the bound-state eigenvalues and eigenfunctions of Schrödinger and other linear operators. All that has been required is a knowledge of the ‘free’, i.e. $V = 0$, Green function and in computer languages which incorporate matrix algebra, the entire program for a simple Schrödinger operator can, typically, be written in less than 20 lines of code. The evaluation of the eigenvalues and eigenvectors requires iteration of a matrix equation and nothing more complicated than matrix multiplications (or loops) need to be performed.

Convergence of the iterations of the method presented is, with the exception of random potential problems, rapid (typical times for calculations on a standard PC are measured in seconds).

Limitations on the accuracy of the method originate primarily from the accuracy of the integration rule used and, as we have seen, even these can be made acceptably small using the very crudest of integration rules with a sufficiently fine grid.

We have presented results here for one- and two-dimensional Schrödinger operators, however we have applied the method successfully to other operators such as Dirac Hamiltonians.

Acknowledgment

I would like to thank Norman Dombey for making helpful comments on an earlier version of this work.

References

- [1] Grimm R and Storer R G 1969 *J. Comput. Phys.* **4** 230–40
- [2] Grimm R and Storer R G 1972 *J. Comput. Phys.* **9** 538–46
- [3] Raphael R B and Tobocman W 1978 *Nucl. Phys. A* **312** 81–96
- [4] Dickinson A S 1972 *J. Comput. Phys.* **10** 162–6
- [5] Landau L D and Lifshitz E M 1977 *Quantum Mechanics (Non-relativistic Theory)* (Oxford: Pergamon)